

Work and efficiency of quantum Otto cycles in power-law trapping potentials

Yuanjian Zheng and Dario Poletti

Singapore University of Technology and Design, 20 Dover Drive, 138682 Singapore

(Received 28 April 2014; revised manuscript received 1 June 2014; published 31 July 2014)

We study the performance of a quantum Otto cycle operating in trapping potentials of different shapes. We show that, while both the mean work output and the efficiency of two Otto cycles in different trapping potentials can be made equal, the work probability distribution will still be strongly affected by the difference in structure of the energy levels. To exemplify our results, we study the family of potentials of the form $V_i(x) \sim x^{2q}$. This family of potentials possesses a simple scaling property that allows for analytical insights into the efficiency and work output of the cycle. We perform a comparison of quantum Otto cycles in various physically relevant scenarios and find that in certain instances, the efficiency of the cycle is greater when using potentials with larger values of q , while in other cases, the efficiency is greater with harmonic traps.

DOI: [10.1103/PhysRevE.90.012145](https://doi.org/10.1103/PhysRevE.90.012145)

PACS number(s): 05.30.-d, 05.70.-a, 05.40.-a

I. INTRODUCTION

The study of thermodynamics at the nanoscale has been a subject of intense interest in recent years (for some recent reviews, see [1,2]). As with classical thermodynamics, one of the main subjects of study is the performance of heat engines. At small scales, heat engines are bound to produce not a deterministic but rather a probabilistic work output because of the relative importance of thermal and quantum fluctuations. In recent years, nonequilibrium work fluctuations have been related to the change of free energy at equilibrium by the Jarzynski's equality [3]. Another notable result, the Crooks equation, relates the forward and backward probabilities of a process [4].

Important recent developments in the study of heat engines include the possibility, both in classical and quantum systems, to externally drive a system such that a physical process is adiabatic despite being executed in a finite time [5–17]. These shortcuts to adiabaticity would allow for the possibility of achieving highly efficient adiabatic-like engines with finite power.

Thus far, quantum thermodynamic cycles and processes have focused primarily on harmonic systems [18–30], with study of anharmonic potentials limited to weak first-order perturbations of a frequency-modulated harmonic oscillator [31], verification of the Jarzynski equality by computation of the nonequilibrium work distribution in a time-varying infinite well [32], and the experimental verification of non-Gaussian behavior [33].

Heat engine cycles using anharmonic traps present very different energy level spacing from harmonic ones, thus resulting in very different work probability distributions. This has important consequences on the quality of the performance of the heat engine, which could be made more or less efficient, or powerful, depending on the shape of the trapping potential used. Furthermore, efficiency and average work output are not the only important figures of merit of a heat engine. The standard deviation of the work is also relevant, as it indicates whether the engine performs more or less consistently (when the standard deviation is smaller or larger, respectively). The comparison between heat engines in different trapping potentials is only fair when the two systems are compared within the same conditions. We will show that whether a

heat engine in a potential performs better than an engine in a different potential depends strongly on the figure of merit analyzed (for example, efficiency) and also on the conditions in which the engines operate (for example, between the same two heat reservoirs).

To exemplify these concepts, we are going to study a particular family of trapping potentials, that of even power-law potentials which are proportional to x^{2q} , where q is a positive integer number and x is the position coordinate of the system. We will show later in the paper that our conclusions pertain to a much wider class of potentials. This family of trapping potentials has a useful scaling property that has been used in [13,14] to engineer counteradiabatic driving protocols. In this paper, we investigate further this class of trapping potentials, which includes both harmonic and anharmonic functions, focusing on utilizing the geometry of the trapping potential to tame the work fluctuations in a quantum heat engine. We examine cycles for which the average work output and efficiency are the same, and also scenarios in which the maximal and minimal temperatures of the quantum gas in the cycle are fixed. We show that not only are the work fluctuations different for different q , but that, depending on the comparative scenarios analyzed, either the harmonic or anharmonic potentials can provide greater efficiency and/or work output.

II. MODEL

The systems we study obey the Hamiltonian

$$\hat{H}(q, \omega_q) = -\frac{\hbar^2}{2m} \frac{\partial^2}{\partial x^2} + \frac{1}{2} m (\omega_q \hat{x})^{2q}, \quad (1)$$

where $q = 1, 2, 3, \dots$ and ω_q represents the magnitude of the generalized trapping potential [13,14]. Note that this generalized trapping potential reverts to the harmonic oscillator for $q = 1$ and to the “infinite” box potential for $q = \infty$. The system undergoes a cycle consisting of four processes [see Figs. 1(a) and 1(b) for a schematic representation]: First an adiabatic compression from a state A_q (q is the anharmonic parameter mentioned earlier), characterized by $\omega_q = \omega'_q$, to B_q , where the amplitude of the trapping is $\omega''_q > \omega'_q$ (no coupling to any thermal bath during this process).

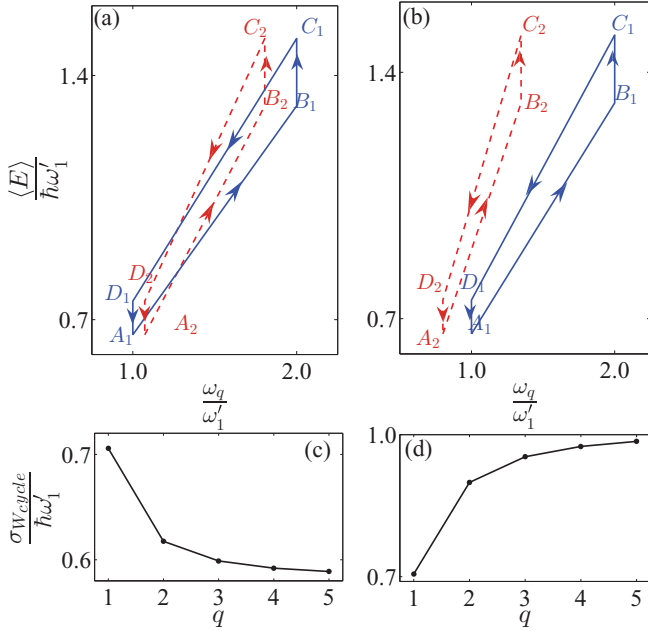


FIG. 1. (Color online) (a),(b) Mean energy $\langle E \rangle$ vs trapping parameter ω_q for a quantum Otto cycle. The continuous blue lines represent the cycle in a harmonic trap ($q = 1$), while the dashed red lines represent a cycle in an anharmonic trap with $q = 2$. (c),(d) Standard deviation of the work distribution $\sigma_{W_{\text{cycle}}}$ vs the anharmonic parameter q . In all the plots, the mean energy at each vertex of the cycle is the same (“matched energies condition”). In (a) and (c) the initial temperature $1/\beta_{A_q}$ is the same for the two different confining potentials, while in (b) and (d) the initial volume, V_{A_q} , is matched. The extremal temperatures for the cycle in a harmonic trap are $1/\beta_{A_1} = 1/2 (\hbar \omega'_1)^{-1}$ and $1/\beta_{C_1} = 5/4 (\hbar \omega'_1)^{-1}$.

This is followed by a heat exchange at constant Hamiltonian parameters (no work is done or received) from B_q to C_q due to a weak coupling to a thermal reservoir. The third process is an adiabatic expansion from C_q to D_q (no coupling to any thermal bath in this process either). Lastly, a heat exchange with the cold reservoir at constant Hamiltonian parameter brings the system back to state A_q . The cycle is fully determined by the choice of ω'_q, ω''_q and by the temperatures $1/\beta_{A_q}$ and $1/\beta_{C_q}$ (we will refer to these last two parameters as the “extremal” temperatures because they are the lowest and highest temperatures achieved in the system).

During the thermodynamic cycle, energy is exchanged under the form of work and heat transfer. When the Hamiltonian parameter ω_q varies from a value ω'_q to ω''_q following a process p , the (inclusive) work is described by the work probability distribution function $P(W_p) = \sum_{m,n} \delta(W_p - E''_m + E'_n) \mathcal{P}^{m,n} P_n$, where E''_m and E'_n are the eigenvalues of, respectively, $\hat{H}(q, \omega'_q)$ and $\hat{H}(q, \omega''_q)$, P_n is the initial thermal probability of occupation of the energy eigenvalue n , and $\mathcal{P}^{m,n}$ is the transition probability from the energy eigenstate n to the eigenstate m relative to the process p (see, for example, [1]). When the system instead undergoes solely a heat exchange, for example between states B_q and C_q , the heat transferred can be computed as the difference of the mean energies $\langle Q_{B_q \rightarrow C_q} \rangle = \langle E \rangle_{C_q} - \langle E \rangle_{B_q}$. And the efficiency of the cycle, η_q , is defined, as per usual, by the ratio of the modulus of

net work done divided by the heat transferred into the system, $\eta_q = -(\langle W_{A_q \rightarrow B_q} \rangle + \langle W_{C_q \rightarrow D_q} \rangle) / \langle Q_{B_q \rightarrow C_q} \rangle$ [34].

While the cycle we study is commonly known as the Otto cycle, it should be noted that in the “classical” Otto cycle, a process in which no work is done or received corresponds to an isochoric process (no change in volume), but in the systems and regimes analyzed here, a process with no work transfer is obtained when the parameters of the Hamiltonian are kept unchanged. In this process, the volume occupied by the gas $V = \sqrt{\langle \hat{x}^2 \rangle}$ does change, as heat is introduced into the system [35].

III. PROPERTIES OF POWER-LAW TRAPPING POTENTIALS

To gain a deeper insight into the problem, we rescale the Hamiltonian using the dimensionless coordinate $X = (\frac{m}{\hbar})^{\frac{1}{1+q}} (\omega_q)^{\frac{q}{1+q}} x$. The dimensionless Hamiltonian $\hat{\mathcal{H}}_q$ is thus

$$\hat{\mathcal{H}}_q = \frac{\hat{H}(q, \omega_q)}{m^{\frac{1-q}{1+q}} (\hbar \omega_q)^{\frac{2q}{1+q}}} = -\frac{1}{2} \frac{\partial^2}{\partial X^2} + \frac{1}{2} \hat{X}^{2q} \quad (2)$$

with eigenvalues $e_{n,q}$. From (2), we observe that the n th energy eigenvalue of \hat{H} , $\varepsilon_n(\omega_q)$, can be written as $\varepsilon_n = m^{\frac{1-q}{1+q}} (\hbar \omega_q)^{\frac{2q}{1+q}} e_{n,q}$.

Now, considering a process in which the Hamiltonian parameter of the trapping potential is changed from ω'_q to ω''_q , we can state, using the aforementioned scaling argument, that the ratio between two energy levels of the same order will only depend on the ratio of parameters of the trapping potential, namely

$$\mu_q \equiv \frac{\varepsilon_n(\omega'_q)}{\varepsilon_n(\omega''_q)} = \left(\frac{\omega'_q}{\omega''_q} \right)^{\frac{2q}{1+q}}. \quad (3)$$

In the following, we will refer to μ_q as the energy ratio parameter. For a given pair of parameters such that $\omega''_q > \omega'_q$ (compression), the energy ratio parameter is bounded: $0 < \mu_q < 1$. Moreover, the scaling properties of the Hamiltonian (1) imply that states are always thermal during adiabatic processes. In fact, for any adiabatic process, where the population of each energy level remains unchanged, an initial thermal state remains thermal so long as $\beta \varepsilon_n(\omega'_q) = \beta' \varepsilon'_n(\omega''_q)$ (where β' has to be the same for every state n) [25]. Using Eq. (3), we can then derive the inverse temperature of the final state $\beta' = \beta \varepsilon_n(\omega'_q) / \varepsilon_n(\omega''_q) = \mu_q \beta$, which is independent of n .

Using the energy ratio parameter μ_q , it is also possible to express the average work of an adiabatic process in a simple form. Considering, for example, the compression from A_q to B_q , the average work is written as

$$\begin{aligned} \langle W_{A_q \rightarrow B_q} \rangle &= \sum_{m,n} [\varepsilon_m(\omega''_q) - \varepsilon_n(\omega'_q)] \mathcal{P}^{mn} P_n^0 \\ &= \left(\frac{1}{\mu_q} - 1 \right) \sum_n \varepsilon_n(\omega'_q) \frac{e^{-\beta \varepsilon_n(\omega'_q)}}{\sum_l e^{-\beta \varepsilon_l(\omega'_q)}} \\ &= \frac{1 - \mu_q}{\mu_q} \langle E \rangle_{A_q}, \end{aligned} \quad (4)$$

where $\langle E_{A_q} \rangle$ is the average energy of the initial state A_q [36]. Furthermore, it is also possible to write the efficiency of the cycle in terms of the energy ratio parameter,

$$\eta_q = 1 - \mu_q, \quad (5)$$

where, in reference to Eq. (4), we have used $\langle W_{A_q \rightarrow B_q} \rangle = (1/\mu_q - 1)\langle E_{A_q} \rangle$, $\langle W_{C_q \rightarrow D_q} \rangle = (\mu_q - 1)\langle E_{C_q} \rangle$, and $\langle Q_{B_q \rightarrow C_q} \rangle = \langle E_{C_q} \rangle - \langle E_{A_q} \rangle/\mu_q$. In classical thermodynamics, the efficiency of the Otto cycle can be written as a function of only the compression ratio $\kappa_q = V_{A_q}/V_{B_q}$ (the ratio between the volume before and after the compression) and of the adiabatic parameter $\gamma = C_p/C_v$ (the ratio between the heat capacity at constant pressure and at constant volume). In this spirit, we write μ_q as a function of the ratio of volumes of the quantum gas by making use of the rescaling of X and the definition of volume V ,

$$\kappa_q = \frac{V_{A_q}}{V_{B_q}} = \left(\frac{\omega'_q}{\omega''_q} \right)^{\frac{q}{1+q}} = \frac{1}{\sqrt{\mu_q}}. \quad (6)$$

This allows us to write the efficiency of the Otto cycle as

$$\eta_q = 1 - \frac{1}{\kappa_q^{\gamma-1}} = 1 - \frac{\beta_{B_q}}{\beta_{A_q}}, \quad (7)$$

which is the same expression as the efficiency of a classical Otto cycle [22] since, for our family of potentials, $\gamma = 3$ [37].

IV. COMPARING ENGINE CYCLES IN DIFFERENT TRAPPING POTENTIALS

Equation (7) shows that the efficiency of the cycle is only a function of the ratio of temperature at the ends of the compression process. However, whether the ratio of the temperatures before and after the compression cycle for one heat engine will be larger or smaller than another will depend on the exact shapes of the potentials and on the operating conditions of the engines. This said, it is thus possible to either compare the efficiency of engine cycles with different values of q or adjust their parameters such that the engine cycles would have the same efficiency. It is also possible to adjust the parameters of engine cycles with different q such that the mean energies at each vertex of the cycle are identical (we will refer to this as the ‘‘matched energies condition’’). This requirement will force both cycles not only to have the same efficiency, but also the same average transfers of heat and work in each process. While the ‘‘matched energies condition’’ guarantees that mean values obtained for the engine cycles are the same, the probability distributions of the work of the cycle, $P(W_{\text{cycle}})$, are bound to be different, due to the different energy level structure of traps with different q . This can be characterized by studying the standard deviation of the work fluctuations, $\sigma_{W_{\text{cycle}}} = \sqrt{\langle W_{\text{cycle}}^2 \rangle - \langle W_{\text{cycle}} \rangle^2}$.

In Figs. 1(a) and 1(b), we represent the Otto cycle in an average energy, $\langle E \rangle$, against the trapping parameter, ω_q , diagram. The blue continuous line represents a cycle for $q = 1$, while the red dashed line is used for $q = 2$. The parameters ω'_q , ω''_q , β_{A_q} , and β_{C_q} have been chosen to fulfill the ‘‘matched energies condition.’’ Note, however, that the matched energies condition does not uniquely define all the parameters. To do

so, we add another, physically relevant, condition: In Figs. 1(a) and 1(c), we have chosen the parameters such that the initial volume V_{A_q} is the same for all q , while in Figs. 1(b) and 1(d) the initial temperatures $1/\beta_{A_q}$ are the same for all q . The standard deviation of the work fluctuations, $\sigma_{W_{\text{cycle}}}$, which characterizes the consistency of the work output, is shown in Figs. 1(c) and 1(d) as a function of q . Here the work probability distribution for a cycle is given by

$$P(W_{\text{cycle}}) = \sum \delta(W_{\text{cycle}} - W_{A_q \rightarrow B_q} - W_{C_q \rightarrow D_q}) \times P(W_{A_q \rightarrow B_q})P(W_{C_q \rightarrow D_q}), \quad (8)$$

where the summation includes all possible values of $W_{A_q \rightarrow B_q}$ and $W_{C_q \rightarrow D_q}$ [34]. Figures 1(c) and 1(d) also clearly show that whether the work fluctuation actually grows or decreases with an increasing anharmonic parameter q depends strongly on the additional matching condition (same initial temperature, volume, or any other relevant physical quantity).

The different work fluctuations for various values of q are rooted in the difference in work probability distributions of the various anharmonic parameters q , which is evident in Fig. 2. In particular, Figs. 2(a) and 2(c) show the work probability distribution for the expansion process, between C_q and D_q . In Fig. 2, we are using the ‘‘matched energies condition’’ and, to uniquely define the parameters of the cycles, we also chose the same temperature $1/\beta_{A_q}$ for both cycles (for the exact

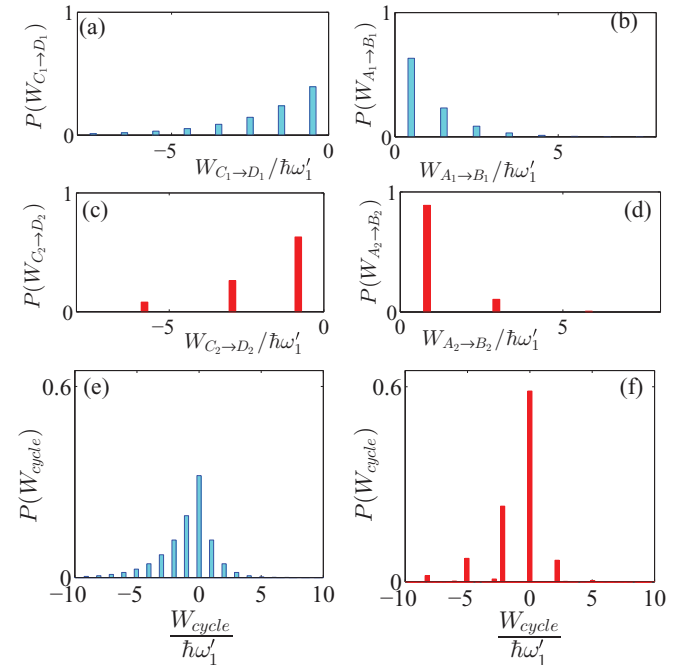


FIG. 2. (Color online) (a),(b) Probability distribution of work, $P(W_p)$, for the adiabatic compression and expansion processes of the cycle in the harmonic trap ($q = 1$). (c),(d) $P(W_p)$ for the compression and expansion processes in the anharmonic trap with $q = 2$. (e),(f) Probability distribution of work for the full quantum Otto cycle for the harmonic (e) and anharmonic, $q = 2$, trap (f). Cycle parameters (corresponding to ‘‘matched energies condition’’ and also matching of the initial temperature $1/\beta_{A_q}$) are $\omega'_1/\omega'_1 = 2$, $\omega'_2/\omega'_1 = 1.392$, $\omega'_2/\omega'_1 = 2.341$, $\beta_{A_1} = \hbar\omega'_1$, and $\beta_{C_1} = 1/4 \hbar\omega'_1$.

parameters, see the caption). Obviously, the histograms are not equidistant in Fig. 2(b) because, unlike in Fig. 2(a), the energy levels are not equidistant. It is also noticeable that the standard deviation in Fig. 2(c) is different from that in Fig. 2(a). These two aspects (the nonequidistance of energy levels and the different variance) are also well represented in Figs. 2(b) and 2(d), where the net work probability distributions of the compression process for $q = 1$ and 2 are depicted, respectively. In Figs. 2(e) and 2(f), we show instead the work probability distribution for the full cycle. We notice clearly that the average work output is negative and that the standard deviation is different in the two cases. We also note the presence of small histograms between much larger ones in Fig. 2(f) but not in Fig. 2(e). This is due to the presence of non-equally-spaced energy levels for $q > 1$.

It is also important to investigate physically relevant scenarios that veer away from the stringent “matched energies condition.” For instance, the extremal temperatures $1/\beta_{A_q}$ and $1/\beta_{C_q}$ could be the same for two engine cycles (because the engines operate between the same two thermal baths). To uniquely define all the parameters of the cycle, two more independent conditions are needed. In Fig. 3, two physically relevant examples are considered: (a) and (c) the case in which the extremal energies ($\langle E_{A_q} \rangle$ and $\langle E_{C_q} \rangle$) are also matched, and (b) and (d) the case in which the extremal volumes (V_{A_q} and V_{C_q}) are identical. As shown in Figs. 3(a) and 3(b), the efficiency of the engine cycles is an increasing function of q

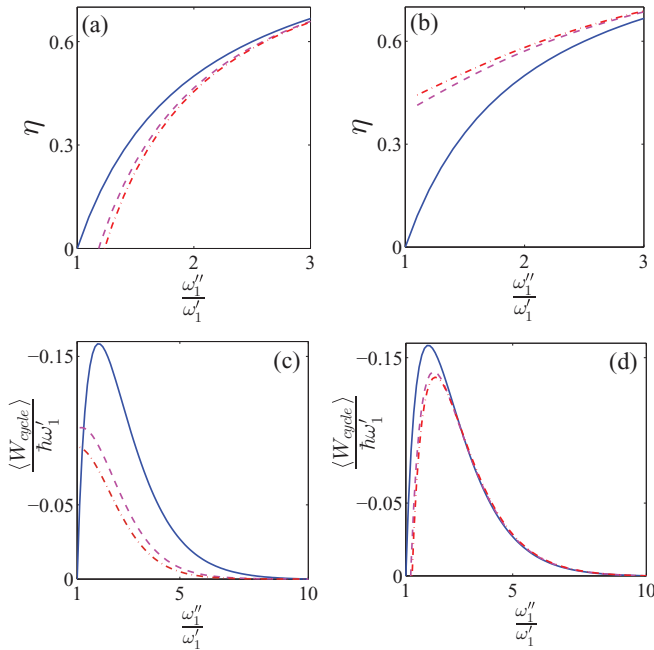


FIG. 3. (Color online) (a),(b) Efficiency of Otto cycles for different values of q vs ω''_1 . (c),(d) Comparison of average work done in a cycle ($\langle W_{\text{cycle}} \rangle$) vs ω''_1 . In all the plots, the continuous blue line is used for $q = 1$, the dashed pink line for $q = 2$, and the dot-dashed red line for $q = 3$. The compared cycles have the same extremal temperatures ($\beta_{A_i} = \beta_{A_j} = 10 \hbar\omega'_1$ and $\beta_{C_i} = \beta_{C_j} = \hbar\omega'_1$ with $i, j = 1, 2, 3$) and, for (a) and (c), matched extremal volumes ($V_{A_i} = V_{A_j}$ and $V_{C_i} = V_{C_j}$ with $i, j = 1, 2, 3$), while in (b) and (d) matched extremal energies ($\langle E_{A_i} \rangle = \langle E_{A_j} \rangle$ and $\langle E_{C_i} \rangle = \langle E_{C_j} \rangle$ with $i, j = 1, 2, 3$).

when the extremal energies are the same, while it decreases with increasing q when the extremal volumes are made the same. Furthermore, Figs. 3(c) and 3(d) shows the net work output of the respective matching conditions, which may in fact be either larger in the harmonic (continuous line) or in the matched anharmonic cases (lines with symbols) depending on the specific matching condition (extremal volumes or extremal mean energies, etc.), and on the value of the matched ω''_1 .

As a last case study, we choose the parameters ω'_q and ω''_q such that the average net work output and the mean initial energy ($\langle E_{A_q} \rangle$) are matched to their corresponding values in the harmonic engine while keeping the extremal temperatures matched for engine cycles with different q . In this case, we expect the efficiency to be dependent on the choice of q , which is clearly seen in Fig. 4(a), where each curve shows the efficiency for different values of q . We note that the figure consists of two separate curves for any given q because the work output, when the two extremal temperatures are fixed, is not a monotonous function of ω''_q , as can be seen in Fig. 4(b). This figure also shows that by fixing the extremal temperatures, there are values of work output that are attainable by the harmonic potential that cannot be generated by anharmonic potentials (to do so would require, for instance, a much larger temperature at C_q or a much lower temperature at A_q). It is for this exact reason that in Fig. 4(a) there exists a central

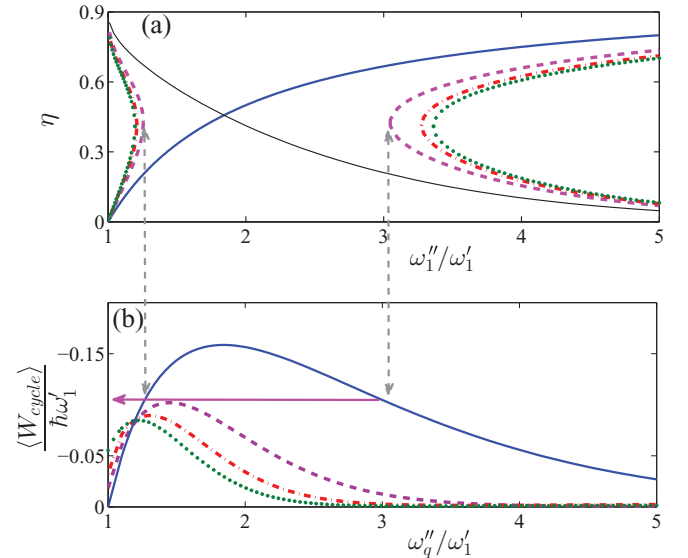


FIG. 4. (Color online) (a) Efficiency of the cycle vs ω''_1 for different anharmonic parameters q . The cycles compared have the same extremal temperatures ($\beta_{A_i} = \beta_{A_j} = 10 \hbar\omega'_1$ and $\beta_{C_i} = \beta_{C_j} = \hbar\omega'_1$ with $i, j = 1, 2, 3, 4$) and perform the same average work ($\langle W_{\text{cycle}} \rangle$). Moreover, the initial mean energy ($\langle E_{A_q} \rangle$) is the same. (b) Average work produced ($\langle W_{\text{cycle}} \rangle$) vs ω''_q for the same initial temperature β_{A_q} and mean energy ($\langle E_{A_q} \rangle$). In (a) and (b) the continuous blue and black lines are used for $q = 1$, the dashed pink line for $q = 2$, the dot-dashed red line for $q = 3$, and the dotted green line for $q = 4$. $\omega'_2/\omega'_1 = 0.9567$, $\omega'_3/\omega'_1 = 0.9137$, $\omega'_4/\omega'_1 = 0.8802$. The pink arrow indicates the maximum work attainable for $q > 1$ (for this matching condition), while the gray, dashed double arrows highlight the boundaries of the region for which engine cycles within a trap with $q > 1$ cannot match the work of the harmonic case.

region of the plot along the ω''/ω'_1 axis for which there are no lines representing the efficiency of engine cycles within an anharmonic trap. In addition, Fig. 4(a) also shows that given a particular ω''_q , the efficiency of all the anharmonic engine cycles (with the same average work and extremal temperatures) can either be always better (for low compressions) or worse (for large compressions) than that of the harmonic cycle. Note that the thin black continuous line in Fig. 4 shows the efficiency of an engine cycle in a harmonic trap which still has the same $\langle E_{A_i} \rangle$ and $\langle W_{\text{cycle}} \rangle$ as the original solid harmonic curve, but is now achieved with a different ω''_q . This analysis of Figs. 4(a) and 4(b) also teaches us that, while a desired amount of net work can be obtained with multiple ω''_q , one particular choice of this value may give the best efficiency.

To understand the generality and applicability of the above results derived for cycles driven by single q parameters, we also investigate the properties of cycles with driving potentials that are composites of multiple x^{2q} terms. These can be seen as a Taylor expansion of cosine potentials typical, for example, of optical lattices. In particular, we consider systems obeying the harmonic-plus-anharmonic Hamiltonian

$$\frac{\hat{H}_{\text{na}}(\lambda, \phi, q)}{\hbar\omega'_1} = -\frac{1}{2} \frac{\partial^2}{\partial X^2} + \lambda \left[\cos(\phi) \frac{\hat{X}^2}{2} + \sin(\phi) \frac{\hat{X}^{2q}}{2q} \right], \quad (9)$$

where $\lambda \in (0, \infty)$ regulates the strength of the trapping potential, $q \neq 1$, and where $\phi \in [0, \pi/2]$ allows to tune the degree of anharmonicity of the trapping potential (while keeping the trapping potential always convex). Note that in the limits $\phi = 0$ and $\phi = \pi/2$, this composite anharmonic potential reverts to the pure harmonic and anharmonic cases, respectively. Using this potential, we calculate the efficiency and work of Otto cycles for a range of anharmonic strengths

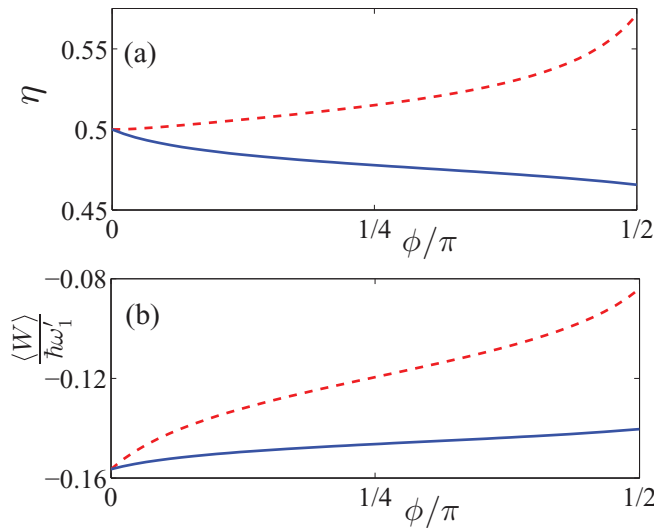


FIG. 5. (Color online) (a) Efficiency and (b) average work of cycles with Hamiltonian (9) ($q = 2$) vs ϕ . The parameters of the anharmonic cycle are computed by matching to a harmonic cycle with $\omega''_i = 2\omega'_1$. Moreover, the temperatures $\beta_{A_i} = \beta_{A_j} = 10\hbar\omega'_1$, $\beta_{C_i} = \beta_{C_j} = \hbar\omega'_1$, and either the extremal volumes (continuous blue line) or extremal average energies (dashed red line) are matched to the harmonic case ($\phi = 0$).

($0 \leq \phi \leq \pi/2$) under identical matching conditions used in Fig. 3 (i.e., matching of either the extremal average energy or extremal volume in addition to operating the engines between the same extremal temperatures $1/\beta_A$ and $1/\beta_C$).

As we can see in Fig. 5, for $q = 2$, both the efficiency and the work are strongly dependent on the matching conditions (blue continuous line for matched extremal energies and red dashed line for matched extremal volumes) and also that work and efficiency are, for the cycles studied, monotonous functions of ϕ . Note also that, while the Otto cycles driven by this composite anharmonic potentials are entirely analogous to those driven by a single q value, the states at points B and D of the composite cycle reached by either adiabatic compression or expansion are, unlike before, nonthermal. This is due to the loss of the unique scale-invariant property of the Hamiltonian, which is only present in the pure x^{2q} potentials. As such, the results derived for the composite potential can only be computed entirely numerically.

V. CONCLUSIONS

We have studied a quantum Otto cycle driven by a particular class of trapping potentials. This family of potentials allows for the investigation of the relative performance of heat engines between harmonic and anharmonic configurations, which paves the way toward optimizing the work fluctuations by detailed design of the trapping geometry. In our analytical treatment, which is made possible by the scaling properties of these potentials, we have found that, regardless of the values of the anharmonic parameter q , all engine cycles share the same expression for the efficiency, which corresponds to the classical expression. However, despite this apparent similarity in the expression for the efficiency, we have shown that the work probability distribution is still strongly affected even when both the average work output and the efficiency of the cycles for different potentials are made identical. Subsequently, we have also analyzed cases in which engine cycles with different potentials are made to operate between the same extremal temperatures, and we studied various physically relevant scenarios for detailed and quantitative comparisons of the different engine cycles; we have found that, if the extremal energies of the cycle are matched, the engines within power-law potentials with $q > 1$ have greater efficiencies than those within a harmonic potential. On the contrary, if the extremal volumes are equal, then engines within the harmonic potential are more efficient. Lastly, we have also shown that, for the case in which the extremal temperatures are the same for the two engines and the parameters are chosen such that the average work output is the same, then, for small compressions, engine cycles within an anharmonic potential are more efficient than cycles within harmonic trapping potentials, while for larger compressions the converse is true. In addition, we have also shown that these results can qualitatively be extended to a more general and wider set of anharmonic trapping potentials that include multiple terms with different values of the anharmonic parameter q .

Given the degree of control and tunability, both in time and in space, of the trapping potentials generated [38,39], these heat engine cycles could be experimentally realized using segmented linear Paul traps.

ACKNOWLEDGMENTS

We are thankful to J. Gong and M. Mukherjee for fruitful discussions, to S. Deffner for clarifications of earlier

work, and to the anonymous referees for useful comments. We acknowledge support from the SUTD start-up grant (Grant No. SRG-EPD-2012-045).

-
- [1] M. Campisi, P. Hänggi, and P. Talkner, *Rev. Mod. Phys.* **83**, 771 (2011).
- [2] U. Seifert, *Rep. Prog. Phys.* **75**, 126001 (2012).
- [3] C. Jarzynski, *Phys. Rev. Lett.* **78**, 2690 (1997).
- [4] G. E. Crooks, *Phys. Rev. E* **60**, 2721 (1999).
- [5] M. Demirplak and S. A. Rice, *J. Phys. Chem. A* **107**, 9937 (2003).
- [6] M. Demirplak and S. A. Rice, *J. Chem. Phys. B* **109**, 6838 (2005).
- [7] M. V. Berry, *J. Phys. A* **42**, 365303 (2009).
- [8] X. Chen, A. Ruschhaupt, S. Schmidt, A. del Campo, D. Guery-Odelin, and J. G. Muga, *Phys. Rev. Lett.* **104**, 063002 (2010).
- [9] E. Torrontegui, S. Ibáñez, S. Martínez-Garaot, M. Modugno, A. del Campo, D. Gury-Odelin, A. Ruschhaupt, Xi Chen, and J. G. Muga, *Adv. At., Mol., Opt. Phys.* **62**, 117 (2013).
- [10] J. W. Deng, Q.-H. Wang, Z. H. Liu, P. Hänggi, and J. B. Gong, *Phys. Rev. E* **88**, 062122 (2013).
- [11] A. del Campo, *Phys. Rev. Lett.* **111**, 100502 (2013).
- [12] A. del Campo, J. Goold, and M. Paternostro, [arXiv:1305.3223](https://arxiv.org/abs/1305.3223).
- [13] C. Jarzynski, *Phys. Rev. A* **88**, 040101(R) (2013).
- [14] S. Deffner, C. Jarzynski, and A. del Campo, *Phys. Rev. X* **4**, 021013 (2014).
- [15] J.-F. Schaff, X.-L. Song, P. Vignolo, and G. Labeyrie, *Phys. Rev. A* **82**, 033430 (2010).
- [16] J.-F. Schaff, X.-L. Song, P. Capuzzi, P. Vignolo, and G. Labeyrie, *Europhys. Lett.* **93**, 23001 (2011).
- [17] M. G. Bason, M. Viteau, N. Malossi, P. Huillery, E. Arimondo, D. Ciampini, R. Fazio, V. Giovannetti, R. Mannella, and O. Morsch, *Nat. Phys.* **8**, 147 (2012).
- [18] O. Abah, J. Roßnagel, G. Jacob, S. Deffner, F. Schmidt-Kaler, K. Singer, and E. Lutz, *Phys. Rev. Lett.* **109**, 203006 (2012).
- [19] J. Roßnagel, O. Abah, F. Schmidt-Kaler, K. Singer, and E. Lutz, *Phys. Rev. Lett.* **112**, 030602 (2014).
- [20] O. Abah and E. Lutz, [arXiv:1303.6558](https://arxiv.org/abs/1303.6558).
- [21] Y. Rezek and R. Kosloff, *New. J. Phys.* **8**, 83 (2006).
- [22] H. T. Quan, Y. X. Liu, C. P. Sun, and F. Nori, *Phys. Rev. E* **76**, 031105 (2007).
- [23] P. Salamon, K. H. Hoffmann, Y. Rezek, and R. Kosloff, *Phys. Chem. Chem. Phys.* **11**, 1027 (2009).
- [24] Y. Rezek, P. Salamon, K. H. Hoffmann, and R. Kosloff, *Europhys. Lett.* **85**, 30008 (2009).
- [25] H. T. Quan, *Phys. Rev. E* **79**, 041129 (2009).
- [26] I. J. Ford, D. S. Minor, and S. J. Binnie, *Eur. J. Phys.* **33**, 1789 (2012).
- [27] P. Talkner, P. S. Burada, and P. Hänggi, *Phys. Rev. E* **78**, 011115 (2008).
- [28] F. Galve and E. Lutz, *Phys. Rev. A* **79**, 055804 (2009).
- [29] J. M. Horowitz, *Phys. Rev. E* **85**, 031110 (2012).
- [30] E. Torrontegui and R. Kosloff, *Phys. Rev. E* **88**, 032103 (2013).
- [31] S. Deffner, O. Abah, and E. Lutz, *Chem. Phys.* **375**, 200 (2010).
- [32] H. T. Quan and C. Jarzynski, *Phys. Rev. E* **85**, 031102 (2012).
- [33] V. Blickle, T. Speck, L. Helden, U. Seifert, and C. Bechinger, *Phys. Rev. Lett.* **96**, 070603 (2006).
- [34] We have neglected, thanks to the weak-coupling approximation, the work done or received by the system during the action of coupling the system itself to the bath.
- [35] As heat is introduced into the system with the Hamiltonian parameters held unchanged, work would have to be done on the system for the gas to occupy the same amount of volume.
- [36] We use the fact that, for an adiabatic process, $\mathcal{P}^{mn} = \delta_{mn}$, where $\delta_{m,n}$ is Kronecker's delta. Note that for a general nonadiabatic Hamiltonian process, the transition probability from eigenstate ϕ_n^0 of the initial Hamiltonian to eigenstate ϕ_m^τ of the final Hamiltonian is given by $\mathcal{P}^{mn} = \int dx_0 \int dx \phi_m^{\tau*}(x) U(x, x_0; \tau) \phi_n^0(x_0)$, where $U(x, x_0; \tau)$ is the unitary time evolution operator.
- [37] This is a consequence of the equation of state $PV = 2\langle E \rangle$, which is valid for the family of trapping potentials considered.
- [38] A. Walther, F. Ziesel, T. Ruster, S. T. Dawkins, K. Ott, M. Hettrich, K. Singer, F. Schmidt-Kaler, and U. Poschinger, *Phys. Rev. Lett.* **109**, 080501 (2012).
- [39] R. Bowler, J. Gaebler, Y. Lin, T. R. Tan, D. Hanneke, J. D. Jost, J. P. Home, D. Leibfried, and D. J. Wineland, *Phys. Rev. Lett.* **109**, 080502 (2012).